HHS Public Access

Author manuscript

Oncogene. Author manuscript; available in PMC 2019 May 02.

Published in final edited form as:

Oncogene. 2019 March ; 38(11): 1905–1919. doi:10.1038/s41388-018-0524-5.

p53-dependent autophagic degradation of TET2 modulates cancer therapeutic resistance

Jixiang Zhang[1,2,*], **Peng Tan**[3,*], **Lei Guo**[1,3,*], **Jing Gong**[4], **Jingjing Ma**[2], **Jia Li**[1], **Minjung Lee**[1], **Shaohai Fang**[1], **Ji Jing**[3], **Gavin Johnson**[1], **Deqiang Sun**[1], **Wen-ming Cao**[5], **Roderick Dashwood**[1,6], **Leng Han**[4], **Yubin Zhou**[3,7,#], **Wei-Guo Dong**[2,#], and **Yun Huang**[1,6,#]

[1]Center for Epigenetics & Disease Prevention, Institute of Biosciences and Technology, Texas A&M University, Houston, TX 77030

[2]Department of gastroenterology, Renmin Hospital of Wuhan University, Wuhan 430060, Hubei Province, China

[3]Center for Translational Cancer Research, Institute of Biosciences and Technology, Texas A&M University, Houston, TX 77030

[4]Department of Biochemistry and Molecular Biology, McGovern Medical School at The University of Texas Health Science Center at Houston, Houston, TX 77030

[5]Department of Breast Medical Oncology, Zhejiang Cancer Hospital, Hangzhou, China, 310022

[6]Department of Molecular & Cellular Medicine, College of Medicine, Texas A&M University, College Station, TX 77843

[7]Department of Medical Physiology, College of Medicine, Texas A&M University, Temple, TX 76504

Abstract

Tumor cells with p53 inactivation frequently exhibit chemotherapy resistance, which poses a longstanding challenge to cancer treatment. Here we unveiled a previously unrecognized role of TET2 in mediating p53-loss induced chemotherapy resistance in colon cancer. Deletion of TET2 in p53KO colon cancer cells enhanced DNA damage and restored chemotherapy sensitivity. By taking a two-pronged approach that combined pharmacological inhibition with genetic depletion, we discovered that p53 destabilized TET2 at protein level by promoting its autophagic degradation. At the molecular level, we further revealed a physical association between TET2 and

[#]Correspondence: dwg@whu.edu.cn; yzhou@ibt.tamhsc.edu; yun.huang@ibt.tamhsc.edu (lead contact).

Author contributions

YH and YZ conceived, directed and oversaw the project. JZ, JM and WD collected CRC samples, p53 mutation analysis and western blotting analysis. JL and DS analyzed the CRC western quantification data. JZ and LG performed the western blotting, doxorubicin / cisplatin treatment, gamma irradiation experiments. JZ and LG performed WST-1, colony forming assays and quantitative real-time PCR analysis. JZ and ML performed the dot-blot assay. JZ and SF performed immunofluorescent staining. JZ generated majority cell lines used in this study. TP provided cell lines lacking autophagosome components and cell cycle blocking experiments. JG and LH performed the mutational analysis in AML patients. GJ and RD provided colon cancer cell lines. JJ, WM, RD and WD provided intellectual inputs. YH and YZ wrote the manuscript with all the other authors participating in discussion, data interpretation and manuscript editing.

[*]These authors contributed equally to the work

p53 that facilitated the nucleoplasmic shuttling of TET2, as well as its recruitment to the autophagosome for degradation. Our study has unveiled a functional interplay between TET2 and p53 during anti-cancer therapy. Our findings establish the rationale for targeting TET2 to overcome chemotherapy resistance associated with mutant p53 tumors.

Keywords

p53; TET2; Autophagy; DNA damage; Doxorubicin; anti-cancer therapy resistance

Introduction

Chemotherapy resistance often arises owing to enhanced DNA repair and failure to apoptose, which is closely associated with mutations in tumor suppressors, such as p53 (1). p53 is a well-known “genome guardian” that maintains the proper cell cycle arrest, DNA repair, and programmed cell death during DNA damage response (2, 3). Drug resistance is one of the reasons accounting for the poor prognosis in patients with p53 inactivating mutations. The correlation between the p53 mutational status and sensitivity to cytotoxic drugs has been confirmed in multiple cancer types (1, 4, 5). Recent exome sequencing in a large cohort of acute myeloid leukemia (AML) patients revealed mutually exclusive mutations in *TP53* and *TET2* (6) (Figure S1), suggesting that cells with genetic lesions in both genes might not undergo malignant transformation or have less survival capability. This finding implies that defining the interplay between p53 and TET2 in tumor cells might yield novel insights into the management of p53 mutant tumors and cancer therapeutic resistance.

Ten-eleven-translocation 2 (TET2) belongs to the TET family of Fe (II)- and α-ketoglutarate-dependent dioxygenases that successively oxidize 5-methylcytosine (5mC) to 5-hydroxymethylcytosine (5hmC), 5-formylcytosine (5fC) and 5-carboxylcytosine (5caC) in the metazoan nucleus (7–11). TET-mediated serial oxidation on 5mC is essential for both active and passive DNA demethylation that paly pivotal roles in various biological process (12, 13). TET2 loss-of-function (LOF) mutations are frequently detected in a large spectrum of hematological malignancies (11, 14–20). Compromised TET enzymatic activities with consequential reduction in its major catalytic product, 5hmC, has been noted in several types of solid tumors (11, 20–23). TET protein is known to regulate genome stability through maintaining DNA damage repair pathways (24), but whether decrease in TET/5hmC levels in tumor cells would affect the DNA damage response induced by anti-cancer therapy remains unclear.

Several protein regulators of TET enzymes have been identified in recent studies (25–27). For example, TET protein levels can be modulated by IDAX, a CXXC domain-containing protein speculated to be originally encoded within TET2 gene and then undergoes chromosome inversion during evolution. IDAX downregulated TET2 protein level through activation of caspase-related pathways (25). In addition, TET protein stability can be modulated by a calcium-dependent protease calpain and P300 mediated acetylation (26, 27). In addition to protease dependent protein degradation pathways, macroautophagy (autophagy hereafter) is a highly conserved cellular degradation and recycling mechanism to

eliminate proteins and organelles to maintain proper cell function (28). Autophagy is considered as a double-edged sword in cancer depending on the context-specific roles during cancer initiation and progression (29).

In the current study, we report that the tumor suppressor p53 regulates TET2 stability through autophagic degradation pathways. In addition, we found that TET2 renders p53-null cancer cells resistant to cancer therapy that targets DNA damage response (e.g. doxorubicin and cisplatin). TET2 inactivation provides a new approach to restore drug sensitivity in p53-null tumors. Our study also calls for cautions in the future application of TET activators in the treatment of cancer. Furthermore, our findings establish a previously unrecognized functional interplay between p53 and TET2, which is critical for drug resistance for tumor cells bearing p53 LOF mutations.

Results

TET2 deletion restores sensitivity of anti-cancer treatment in p53-null tumor cells.

To find the best model system to interrogate the interplay between TET2 and p53 in cancer cells, we examined the protein expression levels of TET2 and p53 in three representative colon cancer cell lines, HTC116, HT29 and SW480. We detected a relatively higher expression of TET2 protein but lower expression of p53 protein in HCT116 cells compared to the other two cell lines HT29 and SW480 (Figure 1A). HCT116 cells are known to display highly aggressive properties with cancer stem cell-like phenotypes (30). We therefore decided to use WT and p53 knockout out (designated p53KO) (generated by Dr. B. Vogelstein's laboratory) (31) HCT 116 cells in this study to further study the interplay between TET2 and p53 during anti-cancer treatment.

We set out to delete TET2 in HCT116 cells (WT and p53KO; Figure 1B) using the CRISPR/Cas9 genome editing method, and then treated these cells with doxorubicin (DXR) in four experimental groups (WT, p53KO, TET2KO, p53KO +TET2KO or DKO). DXR is a commonly used chemotherapy agent in the clinic for cancer treatment (32). DXR acts on cancer cells by interacting with DNA and inhibiting topoisomerase II during DNA replication (33). We used the WST-1 cell viability assay and colony forming assay to monitor cell survival and proliferation (Figure 1C–D) on these cells treated with various does of DXR (0–3.2 μM). Consistent with earlier studies (34), p53KO HCT116 cells exhibited strong resistance to DXR. In the presence of 3.2 μM doxorubicin, approximately 80% of WT HCT116 cells died whereas up to ~50% of p53 KO cells remained viable. Interestingly, in p53KO HCT116 cells further depleted of TET2 (DKO), we observed a pronounced decrease in cell viability and proliferation when compared to p53KO cells. Furthermore, deletion of TET2 in HCT 116 cells showed the most striking decrease in cell survival and proliferation upon DXR treatment (Figure 1C–D). Re-expressing TET2 in TET2KO or DKO HCT 116 cells restored the doxorubicin resistance phenotype (Figure 1D). To confirm this phenotype in vivo, we subcutaneously injected four experimental groups of HCT116 cells (WT, p53KO, TET2KO, and DKO) into the flank of NOD scid gamma mice in the present of DXR treatment, and then monitored tumor growth up to 4 weeks (Figure 1E). Compared to the WT group, mice injected with TET2KO colon cancer cells showed a shrink in tumor size. By contrast, the p53KO group exhibited a significantly larger tumor

volume. However, the DKO group with deletion of both P53 and TET2 displayed an appreciable reduction in tumor size when compared to the p53KO group (Figure 1E). These findings suggested that TET2 is indeed a positive contributor to the chemotherapy resistant feature in p53-null tumor cells in vivo.

To further examine whether this phenotype applies to other chemotherapeutic drugs, we treated HCT116 cells with cisplatin, a potent anticancer agent that inhibits DNA replication (35). We observed similar phonotypes as seen in cancer cells treated with DXR (Figure S1B). To extend our study to other types of cancer cells, we performed the similar experiments in two additional cell lines, SW48 (colon cancer) and MCF7 (breast cancer; Figures S1C–D). Consistent with the scenario seen in HCT116 cells, we found that deletion of TET2 in these engineered p53-null tumor cells could likewise restore their sensitivity to DXR treatment (Figure S1C–D). These data strongly indicate that TET2 renders p53-null tumor cells less sensitive toward chemotherapy agent treatment.

p53-mediated degradation of TET2 enhanced DNA damage in cancer cells

The reciprocal expression patterns of p53 and TET2 in colon cancer cells prompted us to hypothesize that p53 might negatively regulate TET2 gene expression. To quickly test this idea, we compared the endogenous mRNA and protein levels of TET2 in both tumor (p53KO HCT116; Figure 2A) and non-tumor cell lines (HEK293T; Figure 2B), with and without re-expression of FLAG-tagged p53. We found that TET2 protein levels were pronouncedly reduced in both cell types following transient expression of FLAG-p53 without significant alterations in *TET2* mRNA levels (Figure 2A–C). To more rigorously validate this observation, we further utilized a tetracycline-controlled transcriptional activation system to enable inducible and tunable expression of p53 by adding the tetracycline derivative doxycycline (DOX) to both p53KO HCT 116 and HEK293T cells. Upon the addition of increasing doses of doxycycline, we observed a gradual increase in p53 expression with concomitant reduction in the protein levels but not mRNA levels of TET2 (Figure 2D–E). This result was further independently confirmed by immunofluorescent staining of TET2 in HEK293T cells before and after inducible expression of p53 (Figure 2F). Meanwhile, we did not observe a significant change of TET1 mRNA levels in HCT 116 cells with and without p53 expression (Figure S2A), thus ruling out the possibility of functional compensation from the major TET homolog in this cell line.

To further examine whether the resultant reduction in TET2 expression would affect its major catalytic product (5hmC), we performed a dot-blot assay to semi-quantitatively examine 5hmC levels in HEK293T cells with inducible p53 expression system or in p53KO HEK293T cells. We noticed a clear decline in the 5hmC levels following both doxycycline-inducible or transient expression of p53 (Figure 2G). We further confirmed this reciprocal expression pattern of p53 and TET2 in other cancer cell lines (SW48 and MCF7, Figure S2B), as well as in colon cancer patients (Figure 2H). Among the twelve patient samples, three showed detectable p53 mutations (Table S1) and had relatively high TET2 protein levels (Figure 2H). Among the nine patients without p53 mutations, we detected a strong negative correlation between p53 and TET2 protein levels (Figure 2H). Taken together, our

data suggest that p53 can modulate the TET2 protein expression level, likely through a posttranslational mechanism, to affect DNA hydroxymethylation.

Since p53 expression can be rapidly upregulated in tumor cells in response to anti-cancer therapy (e.g., doxorubicin-based chemotherapy or radiotherapy) (36), we asked whether therapeutics-triggered p53 upregulation could reduce TET2 protein levels in HCT116 cells. We monitored TET2 and p53 protein levels in the presence of increasing amounts of doxorubicin (0, 0.2, 0.4, 1, 2 μM) by western blotting (WB). We observed a gradual increase in p53 protein levels with concomitantly reduced TET2 protein levels without a significant alteration in the *TET2* mRNA level (Figure 3A–B). Meanwhile, we did not observe a significant change in the TET1 protein levels in HCT116 cells treated with various doses of doxorubicin (Figure S3A). Similarly, decrease of TET2 protein levels was also observed in HCT116 cells treated with gamma-irradiation ((3 or 6 Gy; Figure 3C) and cisplatin (Figure S3B). As control, we did not observe changes in TET2 protein levels in p53KO HCT116 cells following incubation with doxorubicin (Figure 3D). Similar results were also observed in other cancer cell lines including SW48 and MCF7 (Figure S3C). These data clearly demonstrate that p53 per se could promote TET2 protein degradation during anti-cancer treatment.

Accumulating evidence has suggested that p53 inactivation is closely associated with cancer initiation and progression, partially because those mutant cells are escaped from DNA damage surveillance. Furthermore, it is well known that p53 is significantly upregulated in response to DNA damage response-based cancer treatment. p53-null cancer cells are usually resistant to such treatment due to reduced DNA damage response (34). Recent reports have shown that TET proteins play indispensable roles in the maintenance of genome stability and that deletion of TET proteins could promote DNA damage (24, 37). These findings led us to hypothesize that p53-mediated TET2 degradation is important for safeguarding cells to efficiently respond to DNA damage stress. To test this hypothesis, we first measured double strand DNA break marker, γ-H2AX, in HCT 116 cells treated by gamma-irradiation (Figure 3C), doxorubicin (Figure 3D–E) or cisplatin (Figure S3B). Indeed, we observed significantly increased γ-H2AX protein levels upon irradiation, DXR or cisplatin treatment in WT HCT116 cells (Figure 3E, S3B). By contrast, in p53KO HCT116 cells with intact TET2, we detected a pronounced decrease in γ-H2AX levels compared to WT HCT 116 cells receiving the same treatment, suggesting less DNA damages in p53KO HCT116 cells (Figure 3D–E, Figure S3B). A similar phenotype was also observed in SW48 and MCF7 cells (Figure S3C). Furthermore, the additional deletion of TET2 in p53KO HCT116 cells (DKO) substantially restored the γ-H2AX levels after DXR treatment (Figure 3E). These results converged to support a protective role of TET2 against DNA damage in p53KO HCT116 cells. Together, p53 mediated TET2 degradation is essential for cells responding to DNA damage stress. p53 inactivation maintains relatively higher levels of TET2 in cancer cells to counteract cancer therapy-induced DNA damage, which might contribute to cancer therapeutic resistance in p53 null / mutated cancer cells.

p53 down-regulates TET2 protein levels through autophatic degradation

To further dissect how p53 regulates the protein levels of TET2, we treated cells with inhibitors of proteasome and autophagy pathways in HEK293T cells with inducible expression of p53 (with DOX). We found that treatment of cells with autophagy inhibitors, including 3-methyladenine (3-MA), bafilomycin A1 (BafA1), NH4Cl and chloroquine (CQ), led to prominent TET2 accumulation when p53 expression was induced by DOX (Figure 4A). By contrast, no significant TET2 accumulation was observed in cells treated with a proteasome inhibitor, MG-132. These findings strongly imply that p53 could regulate TET2 protein levels through the autophagic degradation pathway. To further validate this with a genetic approach, we individually depleted key components in the autophagic pathway, including Atg16L1, p62, Beclin 1, and LC3 (Figure 4B). We then compared the TET2 protein levels in those engineered cells in the absence or presence of inducible p53 expression. Following the addition of doxycycline to induce p53 expression, we only observed a significant reduction of TET2 protein levels in WT HEK293T cells, but not in cells lacking autophagic components (Figure 4B). Clearly, both pharmacological and genetic studies converged to support the conclusion that p53 downregulates TET2 protein levels through autophagy-related signaling pathways.

Next, we asked whether p53 is required for the autophagic degradation of TET2. To examine this, we induced autophagy in WT and p53KO HEK293T cells using two well-established protocols: serum-free starvation and rapamycin (Rap) treatment (38). In WT HEK293T cells, we observed increased LC3 and decreased p62 expression upon serum-free starvation (Figure 4C) or rapamycin treatment (Figure 4D), indicating the successful induction of autophagy. Following starvation, we observed a remarkable reduction in TET2 protein levels in native HEK293T cells (with WT p53). Furthermore, autophagy mediated TET2 degradation can be inhibited by the autophagy inhibitor CQ during starvation (Figure 4C). Interestingly, although we observed autophagy induction following treatment with rapamycin or by starvation in p53KO HEK293T cells, the protein levels of TET2 remained largely unaltered, clearly suggesting that p53 is required for autophagy mediated degradation of TET2 (Figure 4C–D).

To further examine whether p53 mediated autophagic degradation of TET2 also occurs in cancer cells, we performed the similar experiment in p53KO HCT116 cells before and after inducible re-expression of p53 (Figure 4E), as well as in HCT116 cells before and after DXR treatment (Figure 4F). In p53KO HCT116 cells, autophagic inhibition by BafA1 exerted no effects on TET2 protein levels. However, following inducible p53 expression in the same p53KO HCT116 cells, BafA1-mediated inhibition of autophagy substantially suppressed TET2 degradation (Figure 4E), a finding that dovetails with the data obtained from HEK293T cells. Next, we asked whether doxorubicin treatment induced decrease of TET2 proteins (Figure 3A) is also mediated by p53 through a similar autophagic mechanism. We monitored the TET2 protein levels in HCT 116 cells in the present of doxorubicin and / or BafA1. We found that Baf1A-mediated autophagic inhibition indeed prevented TET2 protein degradation in HCT116 cells treated with DXR (Figure 4F). In summary, our data clearly suggest that p53 is required for mediating TET2 protein degradation through an autophagic mechanism in both normal and cancer cells.

p53 regulates the nucleocytoplasmic shuttling of TET2

Given that autophagy primarily occurs in the cytoplasm whereas TET2 predominantly resides within the nucleus, we asked whether p53 could impinge on the nucleocytoplasmic shutting of TET2 to promote its autophagic degradation. To better study this process, we knocked out a critical component in the autophagy pathway, Beclin1, in HEK293T cells. This enables us to suppress autophagy for better visualization of protein accumulation in the autophagosome (marked by p62) prior to autophagic degradation of TET2. We first performed immunofluorescence staining of TET2 in WT and beclin1 knockout (Beclin1KO) HEK293T cells. Upon genetic depletion of Beclin 1, we detected a substantial accumulation of TET2 in the cytoplasm. By contrast, in native Hek293T cells, the majority of TET2 was located in the nucleus (Figure 5A). To further biochemically validate this, we separated the cytoplasmic and nuclear fractions and examined the partition of TET2 between these two fractions by immunoblotting in both WT and Beclin1 KO HEK293T cells. We found that deletion of Beclin 1 suppressed p53-mediated TET2 degradation in the cytoplasm (Figure 5B, left) but not for the nuclear fraction (Figure 5B, right). Furthermore, loss of Beclin 1 resulted in cytoplasmic accumulation of TET2 in cells with or without over-expression of p53, suggesting that p53-mediated TET2 deletion mainly occurred in cytoplasm (Figure 5B).

To further examine whether p53 is required for autophagy-mediated cytoplasmic TET2 degradation, we deleted p53 in Beclin1KO HEK293T cells (Figure 5C) and measured the cytoplasmic and nuclear TET2 protein levels in Beclin1 KO or Beclin1 KO + p53KO (DKO) cells. We found a strong TET2 nuclear accumulation in the DKO cells compared with that in Beclin1 single KO HEK293T cells (Figure 5C). Re-expressing p53 in the DKO cells attenuated nuclear TET2 accumulation, suggesting that p53 is essential for the nuclear exit of TET2 to facilitate cytoplasmic degradation (Figure 5C). In parallel, we performed immunostaining experiments to examine whether cytosolic TET2 would co-localize with the autophagosome maker, p62 in Beclin1 KO HE293T cells, so as to demonstrate that the cytosolically accumulated TET2 could be degraded via autophagy after recruitment toward the autophagosome. We used Beclin1 KO HEK293T cells with inducible expression of p53 to prevent TET2 degradation in the cytoplasm and promote its accumulation in autophagosome to increase the signal. We detected a strong co-localization of TET2 and p62 (Figure 5D) in the present of doxycycline (for inducible p53 expression) when compared with cells without doxycycline treatment. The interaction between TET2 and p53 in Beclin1 KO HEK293T cells was further independently confirmed by co-immunoprecipitation (Figure 5E). Furthermore, the interaction between TET2 and p53 did not seem to be affected by the post-translational modifications of p53 (e.g., acetylation and phosphorylation) or by cell cycle blockers (Figure S4A–B).

To determine whether the subcellular localization of p53 could influence autophagic degradation of TET2, we resorted to several well-studied p53 mutants that have distinct distribution patterns: R175H (cancer-associated mutant without affecting its nuclear and cytoplasmic location) (39), K305A (cytoplasmic accumulation) (40), and L348A/L350A (nuclear accumulation) (41) (Figure 6A). In p53KO cells, notable TET2 degradation was observed following the re-expression of WT p53 or the R175H mutant. However, in p53KO cells expressing the K305A or L348A/L350A mutants, we did not detect a significant

decrease in TET2 protein levels (Figure 6A). Next, we separated the nuclear and cytoplasmic fractions of cells expressing WT or mutant p53, and further monitored TET2 protein levels using western blotting. We observed a strong nuclear accumulation of TET2 in p53 KO cells expressing the K305A or P53-L348A/L350A mutants (Figure 6B), but not in those expressing WT p53 or the R175H mutant. This was further confirmed by immunofluorescent staining (Figure 6C). These results suggest that proper subcellular localization of p53 is essential for autophagy-mediated TET2 degradation. Together, our data established that p53 can interact with TET2 in the cytoplasm to facilitate its recruitment to the autophagosome, thereby promoting the autophagic degradation of TET2.

Discussions

It is well known that tumors bearing genetic alterations in p53 are commonly aggressive and resistant to anti-cancer treatment. In this study, we identified a novel interplay between p53 and TET2 during anti-cancer treatment. We discovered a negative correlation between p53 and TET2 protein levels in colon cancer cell lines, as well as in primary colon tumor samples. We demonstrated that p53 facilitates the autophagic degradation of TET2 in both tumor (HCT116, SW48 and MCF7) and non-tumor cell lines (HEK293T). Furthermore, we showed that such negative correlation between p53 and TET2 is essential for balancing the DNA damage response when cells are challenged with extra-cellular stresses, such as anti-cancer therapy (e.g., doxorubicin, cisplatin and gamma-irradiation treatment). Mechanistically, we revealed that p53 is required for autophatic degradation of TET2 by promoting the shuttling of nuclear TET2 toward the cytoplasmic autophagosome. Deletion of p53 resulted in the disconnection between TET2 and autophagosome, which led to the increase of cellular survival when responding to DNA damage and therefore promoted anti-cancer therapy resistance in p53-null tumor cells (Figure 7). Our study establishes the rationale for targeting TET2 as a potential strategy for overcoming anti-cancer treatment resistance associated with deregulated p53.

Previous studies have shown that TET2 is a tumor suppressor gene. Genetic alteration of *TET2* are frequently observed in hematological malignancies. TET2 loss or downregulation is implicated in tumor initiation and invasion (20, 42). Furthermore, protective roles of the TET protein family have been reported by regulating DNA damage response during cellular malignant transformation (24, 37, 43). Surprisingly, in our study, TET2 mediated protective effect on DNA damage seems to act as a “double edged sword” during anti-cancer treatment. When tumor cells (e.g., HCT116, SW48 and MCF7) bearing WT p53 are treated with chemotherapy reagents (e.g, doxorubicin or cisplatin), p53-mediated TET2 degradation induces substantial DNA damage, leading to increased tumor cell death. Conversely, in p53KO HCT 116 cells, the high level of TET2 protein protects the genome from chemotherapy induced DNA damage and subsequently promotes cell survival (Figure 7). Thus, TET2 depletion could at least partially overcome anti-cancer treatment resistance in p53KO tumor cells.

To date, autophagy-mediated protein degradation is mainly focused on cytoplasmic components. Recently, Dou *et al.* illustrated LC3-mediated nuclear lamin B1 degradation in autophagosome (44), which is essential for preventing cells from malignant transformation

to safeguard against tumorigenesis. Our studies demonstrated that TET2 as a nuclear protein can be translocated from nucleus to cytoplasm via p53 through direct interaction, thereby trapping TET2 in the cytosol to promote its association with autophagosome for ultimate degradation. The protein stability of TET2 can be modulated by several pathways that involve caspase (25), calpains (26) and p300 mediated acetylation (27). Our study provides an additional regulatory mechanism with respect to the posttranslational regulation of TET2 in response to extracellular stress imposed by cancer therapeutics in the context of a specific genetic background (e.g., p53-null tumor cells). Our study points to the exciting possibility that TET2 inhibition might serve as a promising strategy to reduce cancer therapeutic resistance in p53-null tumors. Our findings also call for extra cautions during the future development and application of TET activators/agonists in the treatment of cancer.

Materials and methods

Cell culture

HEK293T, HCT 116, SW480, HT29, SW48 and MCF-7 cell lines were purchased from ATCC and cultured in Dulbecco's modified Eagle's medium (Corning, Manassas, VA, USA) with 10% fetal bovine serum (Omega, Tarzana, CA, USA), 1% antibiotics (100 IU penicillin and 100 μg/mL streptomycin) and 2mM L-glutamine with 1mM 2-mercaptoethanol in a humidified incubator at 37°C with 5% CO_2. The medium was changed every two days and cells were split when reaching a confluence of 80–90%.

Chemicals

Doxycyclin (D9891), Doxorubicin (D1515), MG-132 (M7449), 3-Methyladenine (M9281), Chloroquine (C6628), Bafilomycin A1 (B1793), Cisplatin (1134357) and rapamycin (R8781) were purchased from Sigma-Aldrich (St Louis, MO, USA). Puromycin and Zeocin were purchased from Thermo Fisher Scientific (Grand Island, NY, USA). Cell cycle blockers, including MK-1775 (21266), Flavopiridol (10009197), Palbociclib (16273), were purchased from Cayman Chemical Company.

Plasmids

Human TET2, p53, Atg16L1, Beclin1, LC3A, LC3B, p62 were cloned from HEK293T cells using reverse transcription PCR. p53 mutants (R175H, K305A and L348A+L350A) were constructed by using the QuikChange site-directed mutagenesis kit (Catalog #200523) from Agilent Inc.. For transient expression in mammalian cells, the cDNA encoding human TET2 was cloned into a modified pcDNA3-Flag-Dest-B vector. The CRISPR/Cas9 genome editing construct PX459 (62988; Addgene) was used for sgRNA-directed knockout of TET2, p53, Atg16L1, Beclin1, LC3, p62.

TET2 sgRNA-1: caccgTGGAGAAAGACGTAACTTCG

TET2 sgRNA-2: caccgCAGGACTCACACGACTATTC

p53 sgRNA-1: caccgCCATTGTTCAATATCGTCCG

p53 sgRNA-2: caccgCCCCGGACGATATTGAACAA

Atg16L1 sgRNA: caccgAGATGTGGCGCTTCCAGCGG

Beclin1 sgRNA: caccgGGACACGAGTTTCAAGATCC

p62 sgRNA : caccgCACCGTGAAGGCCTACCTTC

LC3 sgRNA: caccgACCTCCTTACAGCGGTCGGC

The sgRNA-containing plasmids were transfected into HEK293T cells and subjected to puromycin selection (2 μg ml^{-1}) for 2–4 days. Survival clones were then seeded into 96-well plates and later expanded to 24-well plates for maintenance in the presence of 1 μg ml^{-1} puromycin. The gene disruption was confirmed by western blotting. All the plasmid information was listed in Table S2.

Xenograft models

1×10^6 HCT116 cells were suspended in 50 μl PBS mixed with an equal volume of pathogen-free BD Matrigel. Basement Membrane Matrix were implanted subcutaneously into the flank of NOD scid gamma mice (6–8 weeks old, Jackson laboratory, 005557). Doxorubicin was injected at 4mg/kg every two days starting at day 4 after tumor implantation for 4 weeks via intraperitoneal injection. The tumor volume was measured with a caliper every week according to the formula: 0.52 × length × width × height. All animal experiments in this study were approved by the Texas A&M University Review Board.

Human Subjects

A total of 12 tumor samples were collected from patients with colorectal cancer (CRC) at the Renmin Hospital of Wuhan University. Detailed clinical and pathological data were summarized in Table 1. All tissue samples were obtained from patients with approval from Institutional Review Board of Renmin hospital of Wuhan University China (No. 2018K-C007). Informed consent was obtained from the individual patient.

P53 exome sequencing

p53 exome sequencing was performed by following the manufacturer's protocols from Tsingke Biological Technology Inc. Genomic DNA was isolated from freshly frozen CRC tissues using the Trelief TM Animal Genomic DNA Kit (catalog #TSP201–200) and the Maxwell® 16 MDx Instrument (Promega Corp., Madison, WI, USA). Purified genomic DNA was then quantified using the Qubit® dsDNA HS Assay Kit (catalog #Q32851) and a Qubit 2.0 fluorometer (Thermo Fisher Scientific, Waltham, MA, USA). Seven pairs of primers were designed to capture the p53 exome:

p53-1-F: CCTCCTCCCCAACTCCATTTC,

p53-1-R: CCGAGAGCCCGTGACTCAGA;

p53-2-3-4-F: GGAAGCCGAGCTGTCTCAGACA,

p53-2-3-4-R: GGGGATACGGCCAGGCAT;

p53-5-6-F: GGTGTAGACGCCAACTCTCTCTAGC,

p53-5-6-R: GGCCACTGACAACCACCCTTAA;

p53-7-F: GAGGCTGAGGAAGGAGAATGG,

p53-7-R: GCCCAGGGGTCAGAGGCA;

p53-8-9-10-F: AAGGGTGGTTGGGAGTAGATGG,

p53-8-9-10-R: GCAGGCTAGGCTAAGCTATGATG;

p53-11-F: AAGTCAGCTGTATAGGTACTTGAAGTGC,

p53-11-R: TCAGCTGCCTTTGACCATGAA;

p53-12-F: ACCATCTTGATTTGAATTCCCG,

p53-12-R: CCCCAGCCCACACTCATTG.

Exome sequencing was performed using the BigDye Terminator v3.1 Cycle Sequencing Kit (Thermo Fisher, catalog #4337458) on an ABI 3730×l DNA analyzer (Thermo Fisher Scientific, Waltham, MA, USA).

Nuclear and cytoplasmic proteins extraction

Cells (1×10^7) were resuspended with cytoplasmic and nuclear protein lysis buffer A (10mM HEPES, pH 7.9, 10mM KCl, 1mM DTT, 0.1mM EDTA) supplemented with protease inhibitor and phosphatase inhibitor cocktail (Gendeport, Barker, TX, USA) on ice for 25 min. Next, 5 μl of 10% NP-40 was added into the samples and incubated on ice for another 2 min. After centrifugation at 5,000 rpm for 3 min, the supernatant was collected as cytoplasmic extracts. The nuclear pellet was further cleared by centrifugation at 12,000 rpm for 3 min followed by removal of supernatant. The pellet was further lysed by 50 μl of cytoplasmic and nuclear protein lysis buffer C (10mM HEPES, pH 7.9, 400nM NaCl, 1mM EDTA, 1mM DTT). After incubation for 1 h at 4°C, the samples were centrifuged at 12,000 rpm for 15 min and the supernatant (nuclear fractions) was collected.

Western Blotting and Co-immunoprecipitation

Tumor samples collected from CRC patients were flash-frozen in liquid nitrogen and then lysed in ice-cold lysis buffer (20mM Tris-HCl pH 7.8, 150mM NaCl, 2mM EDTA pH 8.0, 1% NP40, 10% glycerol, supplemented with 10 mM NaF, 10 mg/mL Leupeptin, 200mM Na_2VO_4, 5mM PMSF, and Aprotinin) (Sigma-Aldrich). Homogenization was performed on ice with a POLYTRON® system PT 1200 E (Kinematica). Lysates were centrifuged at 13.000 rpm 4°C for 30 min and the supernatants were collected. Cells were lysed on ice by using RIPA lysis buffer (50mM Tris-HCl pH 7.4, 1% NP-40, 0.5% Na-deoxycholate, 0.1% SDS, 150mM NaCl, 2mM EDTA, 50Mm NaF) supplemented with protease inhibitor and phosphatase inhibitor cocktail (Gendeport, Barker, TX, USA). The total protein concentration was measured by the BCA protein assay kit (Thermo, Rockford, IL, USA). The protein extractions were denatured by SDS-sample buffer and incubated at 95°C for 10 min. The denatured protein mixture was subjected to SDS-PAGE, subsequently transferred to nitrocellulose membranes (Millipore, Billerica, MA, USA), and blocked with 5% non-fat milk in Tris-buffered saline pH 7.6 containing 0.1% Tween-20. Then the membranes were probed with the corresponding primary antibodies overnight at 4°C. After washing with TBS-T buffer for three times (10 min for each wash at room temperature), the membranes were incubated with an anti-rabbit secondary antibody (1:10000, sigma, Cat# 7074) or anti-mouse secondary antibody (1:3000, Cell Signaling Technology, Cat# 7076) for 1 h at room

temperature followed by washing with TBST three times (10 mins for each wash at room temperature). The antigen–antibody complexes were detected using West-Q Pico Dura ECL Solution (Gendeport, Barker, TX, USA). The intensities of protein bands on the films were quantified by scanning densitometry using the Image J software (NIH).

For co-immunoprecipitation cells were lysed on ice with CHAPS lysis buffer (Gendeport, Barker, TX, USA) including 50mM Tris-HCl (pH 7.4), 110mM NaCl, 5mM EDTA and 1% CHAPS, supplemented with protease inhibitors and phosphatase inhibitors cocktail (Gendeport, Barker, TX, USA) for 5 min, and then subjected to centrifugation at 12,000rpm at 4°C for 5 min. Subsequently, cell lysate was incubated with indicated antibodies and magnetic A/G beads (Thermo Fisher Scientific) overnight at 4°C. The beads were washed with the wash buffer (50 mM Tris–HCl, pH7.5, 150 mM NaCl, 1 mM EDTA and 0.5% Triton X-100, containing 10 mg/ml pepstatin A, 10 mg/ml leupeptin and 1 mM PMSF) and heated in SDS loading buffer at 95°C for 5 min. Then the cell lysate was subjected to SDS-PAGE.

The primary antibodies used in the study include: mouse anti-TET2 (1:500, Active motif, Cat#61389), rabbit anti-TET1 (1:500, Active Motif, Cat#61443), mouse anti-p53 (1:2500, Santa Cruz, Cat# sc-126), mouse anti-Flag (1:3000, Sigma, Cat#F1804), mouse anti-HA (1:1000, Santa Cruz, Cat#sc-7392), rabbit anti-ATG16L1 (1:1000, Cell Signaling Technology, Cat#8089), rabbit anti-Beclin1 (1:1000, Cell Signaling Technology, Cat#3495), rabbit anti-p62 (1:1000, Santa Cruz, Cat#sc-28359), rabbit anti-LC3 (1:1000, Cell Signaling Technology, Cat#12741), rabbit anti-γH2AX (1:1000, Cell Signaling Technology, Cat#9718), mouse anti-Tubulin (1:2000, Sigma, Cat#TG074), rabbit anti-LaminB1 (1:3000, Abcam, Cat#ab16048), and rabbit anti-GAPDH (1:10000, Cell Signaling Technology), rabbit anti Phospho-p53-Ser15 (1:1000, Cell Signaling Technology) and rabbit anti Acetyl-p53-Lys382 (1:1000, Cell Signaling Technology).

RNA extraction, reverse transcription and quantitative real-time PCR

Total RNA was extracted with the TRIzol RNA isolation reagent (Thermo Fisher Scientific, Grand Island, NY, USA). cDNA synthesis was carried out by using the amfiRivert Platinum One cDNA Synthesis Master Mix (Gendeport, Barker, TX, USA). Quantitative real-time PCR were performed using amfiSure qGreen q-PCR Master Mix without ROX (Gendeport, Barker, TX, USA).

The primer sequences were listed as follows:

p53 forward: 5’-CAGCACATGACGGAGGTTGT-3’,

p53 reverse: 5’-TCATCCAAATACTCCACACGC-3’;

TET2 forward: 5’-ATACCCTGTATGAAGGGAAGCC-3’,

TET2 reverse: 5’-CTTACCCCGAAGTTACGTCTTTC-3’;

GAPDH forward: 5’-GCACCGTCAAGGCTGAGAAC-3’,

GAPDH reverse: 5’-TGGT GAAGACGCCAGTGGA-3’.

The Dot blot assay

Genomic DNA from cells was isolated using NucleoSPIN® Tissue (Macherey-Nagel, Bethlehem, PA, USA). 5μg of DNA was denatured in 1M NaOH, 25mM EDTA at 95°C for 10 min. Then the samples were neutralized with ice-cold 2 M ammonium acetate (pH 7.0) followed by twofold serial dilution of DNA samples, with each being spotted on a nitrocellulose membrane in an assembled Bio-Dot apparatus (Bio-Rad). DNA samples were filtered under vacuum pressure and the membrane was washed with 2×SSC buffer, air-dried at room temperature for 20 min and vacuum-baked at 80°C for 2 h. Next, the membrane was blocked in 5% milk at room temperature for 1 hr and incubated with a rabbit anti-5-hmC primary antibody (1:5000, Active motif, Cat#39769) overnight at 4°C. The membrane was washed with TBST buffer for 10 min three times and then incubated with an anti-rabbit secondary antibody (1:10000, sigma, Cat#7074) for 1 hr at room temperature. Next, the membrane was washed for 10 min three times and visualized by chemiluminescence with West-Q Pico Dura ECL Solution (Gendeport, Barker, TX, USA). Finally, the membrane was washed with TBST and stained with 0.02% methylene blue in 0.3 M sodium acetate (pH 5.2) to ensure equal spotting of total DNA on the membrane.

Immunofluorescent staining

Cells (2×10^6 / ml) were seeded and grown on sterile cover slips in 12-well plates. Following treatment, cells were washed with warm PBS and fixed in 4% paraformaldehyde for 10 min. Fixed cells were then washed three times with PBS, permeabilized with 0.2% Triton X-100 for 15 min and blocked in 5% BSA for 30 min. Next, cells were incubated with primary antibodies: mouse anti-TET2 (1:100, Active motif, Cat#61389), mouse anti-p53 (1:500, Santa Cruz, Cat#sc-126) and rabbit anti-p62 (1:1000, Santa Cruz, Cat#sc-28359) followed by washing three times with PBS, and incubation with Alexa Fluor® 488 goat anti-mouse (Invitrogen, 1:2000, Cat#A11001) or an Alexa Fluor® 568 goat anti-rabbit (Invitrogen, 1:2000, Cat#11011) secondary antibody for 1 h at room temperature. Cells were then washed 3 times with PBS and mounted with Prolong Gold (Life Technologies). Cells were imaged with 40×oil lens on an inverted Nikon Eclipse Ti-E microscope customized with A1R confocal imaging modules and the images were analyzed by NIS-Elements software (Nikon) or Image J (NIH).

Cell viability assay

WST-1 (Sigma-Aldrich, Cat# 05015944001) was used to quantitatively assess cell viability. Cells (5×10^3) were seeded into 96-well plates. On day 2, the medium was replaced and cells were cultured in fresh medium containing doxorubicin at different concentrations for 12 h, 24 h, 36 h, 48 h and 60h. Then 10 μl WST-1 solution with 90 μl DMEM medium were added to each well, and cells were incubated at 37°C for 1h. The absorbance at 450 nm was determined by using a Cytation 5 microplate reader (BioTek, Winooski, USA). DMEM containing 10% WST-1 was used as negative control.

Colony formation assay

Cells (3×10^4 cells) were seeded in 48-well plates. The next day, corresponding treatments were applied. Cells were then washed with PBS two times 5 days later. After fixation with

100% methanol at room temperature for 15 min and wash with PBS two times, the colonies were stained using crystal violet (0.25%, Sigma-aldrich, Cat#C3886) at room temperature for 5 min and photographed.

Statistical Analysis

The mutation status in AML patients were obtained from Table S5 in ref 6. The exclusive analysis was calculated by Fisher's test. All the western blotting analyses were performed for at least three independent times. Data were expressed as the mean ± SD. The difference among 3 or more groups was determined by ANOVA, and the difference between two groups was analyzed by the Student's t-test using the SPSS 17.0 for Microsoft Windows (SPSS Inc., Chicago, IL, USA). A value of $p<0.05$ was considered to indicate a statistically significant result. No randomization and blinding was used in this study.

Supplementary Material

Refer to Web version on PubMed Central for supplementary material.

Acknowledgements

This work was supported by grants from Cancer Prevention and Research Institute of Texas (RR140053 to YH, to RP170660 to YZ, RR150085 to LH), the Innovation Award from American Heart Association (16IRG27250155 to YH), the John S. Dunn Foundation Collaborative Research Award (to YH), the Center for Translational Environmental Health Research (CTEHR) Seed Grant to YH, the National Institute of Health grants (R01GM112003 to YZ), the Welch Foundation (BE-1913 to YZ), the American Cancer Society (RSG-16-215-01-TBE to YZ), and by an allocation from the Texas A&M University startup funds (YH).

References

1. Hientz K, Mohr A, Bhakta-Guha D, Efferth T. The role of p53 in cancer drug resistance and targeted chemotherapy. Oncotarget. 2016.
2. Bieging KT, Mello SS, Attardi LD. Unravelling mechanisms of p53-mediated tumour suppression. Nat Rev Cancer. 2014;14(5):359–70. [PubMed: 24739573]
3. Muller PA, Vousden KH. p53 mutations in cancer. Nat Cell Biol. 2013;15(1):2–8. [PubMed: 23263379]
4. Shetzer Y, Solomon H, Koifman G, Molchadsky A, Horesh S, Rotter V. The paradigm of mutant p53-expressing cancer stem cells and drug resistance. Carcinogenesis. 2014;35(6):1196–208. [PubMed: 24658181]
5. Bergamaschi D, Gasco M, Hiller L, Sullivan A, Syed N, Trigiante G, et al. p53 polymorphism influences response in cancer chemotherapy via modulation of p73-dependent apoptosis. Cancer Cell. 2003;3(4):387–402. [PubMed: 12726864]
6. Papaemmanuil E, Cazzola M, Boultwood J, Malcovati L, Vyas P, Bowen D, et al. Somatic SF3B1 mutation in myelodysplasia with ring sideroblasts. N Engl J Med. 2011;365(15):1384–95. [PubMed: 21995386]
7. Tahiliani M, Koh KP, Shen Y, Pastor WA, Bandukwala H, Brudno Y, et al. Conversion of 5-methylcytosine to 5-hydroxymethylcytosine in mammalian DNA by MLL partner TET 1. Science. 2009;324(5929):930–5. [PubMed: 19372391]
8. Koh KP, Yabuuchi A, Rao S, Huang Y, Cunniff K, Nardone J, et al. Tet1 and Tet2 regulate 5-hydroxymethylcytosine production and cell lineage specification in mouse embryonic stem cells. Cell Stem Cell. 2011;8(2):200–13. [PubMed: 21295276]
9. He YF, Li BZ, Li Z, Liu P, Wang Y, Tang Q, et al. Tet-mediated formation of 5-carboxylcytosine and its excision by TDG in mammalian DNA. Science. 2011;333(6047):1303–7. [PubMed: 21817016]

10. Ito S, Shen L, Dai Q, Wu SC, Collins LB, Swenberg JA, et al. Tet proteins can convert 5-methylcytosine to 5-formylcytosine and 5-carboxylcytosine. Science. 2011;333(6047):1300–3. [PubMed: 21778364]
11. Ko M, Huang Y, Jankowska AM, Pape UJ, Tahiliani M, Bandukwala HS, et al. Impaired hydroxylation of 5-methylcytosine in myeloid cancers with mutant TET2. Nature. 2010;468(7325):839–43. [PubMed: 21057493]
12. Hashimoto H, Liu Y, Upadhyay AK, Chang Y, Howerton SB, Vertino PM, et al. Recognition and potential mechanisms for replication and erasure of cytosine hydroxymethylation. Nucleic Acids Res. 2012;40(11):4841–9. [PubMed: 22362737]
13. Inoue A, Zhang Y. Replication-dependent loss of 5-hydroxymethylcytosine in mouse preimplantation embryos. Science. 2011;334(6053):194. [PubMed: 21940858]
14. Bejar R, Stevenson KE, Caughey BA, Abdel-Wahab O, Steensma DP, Galili N, et al. Validation of a prognostic model and the impact of mutations in patients with lower-risk myelodysplastic syndromes. J Clin Oncol. 2012;30(27):3376–82. [PubMed: 22869879]
15. Delhommeau F, Dupont S, Della Valle V, James C, Trannoy S, Masse A, et al. Mutation in TET2 in myeloid cancers. N Engl J Med. 2009;360(22):2289–301. [PubMed: 19474426]
16. Tefferi A, Lim KH, Abdel-Wahab O, Lasho TL, Patel J, Patnaik MM, et al. Detection of mutant TET2 in myeloid malignancies other than myeloproliferative neoplasms: CMML, MDS, MDS/MPN and AML. Leukemia. 2009;23(7):1343–5. [PubMed: 19295549]
17. Quivoron C, Couronne L, Della Valle V, Lopez CK, Plo I, Wagner-Ballon O, et al. TET2 inactivation results in pleiotropic hematopoietic abnormalities in mouse and is a recurrent event during human lymphomagenesis. Cancer cell. 2011; 20(1):25–38. [PubMed: 21723201]
18. Lemonnier F, Couronne L, Parrens M, Jais JP, Travert M, Lamant L, et al. Recurrent TET2 mutations in peripheral T-cell lymphomas correlate with TFH-like features and adverse clinical parameters. Blood. 2012;120(7):1466–9. [PubMed: 22760778]
19. Abdel-Wahab O, Mullally A, Hedvat C, Garcia-Manero G, Patel J, Wadleigh M, et al. Genetic characterization of TET1, TET2, and TET3 alterations in myeloid malignancies. Blood. 2009;114(1):144–7. [PubMed: 19420352]
20. Huang Y, Rao A. Connections between TET proteins and aberrant DNA modification in cancer. Trends Genet. 2014;30(10):464–74. [PubMed: 25132561]
21. Yang H, Liu Y, Bai F, Zhang JY, Ma SH, Liu J, et al. Tumor development is associated with decrease of TET gene expression and 5-methylcytosine hydroxylation. Oncogene. 2012.
22. Thienpont B, Steinbacher J, Zhao H, D'Anna F, Kuchnio A, Ploumakis A, et al. Tumour hypoxia causes DNA hypermethylation by reducing TET activity. Nature. 2016;537(7618):63–8. [PubMed: 27533040]
23. Nakagawa T, Lv L, Nakagawa M, Yu Y, Yu C, D'Alessio AC, et al. CRL4(VprBP) E3 ligase promotes monoubiquitylation and chromatin binding of TET dioxygenases. Mol Cell. 2015;57(2): 247–60. [PubMed: 25557551]
24. An J, Gonzalez-Avalos E, Chawla A, Jeong M, Lopez-Moyado IF, Li W, et al. Acute loss of TET function results in aggressive myeloid cancer in mice. Nat Commun. 2015;6:10071. [PubMed: 26607761]
25. Ko M, An J, Bandukwala HS, Chavez L, Aijo T, Pastor WA, et al. Modulation of TET2 expression and 5-methylcytosine oxidation by the CXXC domain protein IDAX. Nature. 2013;497(7447): 122–6. [PubMed: 23563267]
26. Wang Y, Zhang Y. Regulation of TET protein stability by calpains. Cell Rep. 2014;6(2):278–84. [PubMed: 24412366]
27. Zhang YW, Wang Z, Xie W, Cai Y, Xia L, Easwaran H, et al. Acetylation Enhances TET2 Function in Protecting against Abnormal DNA Methylation during Oxidative Stress. Mol Cell. 2017;65(2): 323–35. [PubMed: 28107650]
28. Guo JY, Xia B, White E. Autophagy-mediated tumor promotion. Cell. 2013;155(6):1216–9. [PubMed: 24315093]
29. White E Deconvoluting the context-dependent role for autophagy in cancer. Nat Rev Cancer. 2012;12(6):401–10. [PubMed: 22534666]

30. Yeung TM, Gandhi SC, Wilding JL, Muschel R, Bodmer WF. Cancer stem cells from colorectal cancer-derived cell lines. Proc Natl Acad Sci U S A. 2010;107(8):3722–7. [PubMed: 20133591]
31. Boyer J, McLean EG, Aroori S, Wilson P, McCulla A, Carey PD, et al. Characterization of p53 wild-type and null isogenic colorectal cancer cell lines resistant to 5-fluorouracil, oxaliplatin, and irinotecan. Clin Cancer Res. 2004;10(6):2158–67. [PubMed: 15041737]
32. Tacar O, Sriamornsak P, Dass CR. Doxorubicin: an update on anticancer molecular action, toxicity and novel drug delivery systems. J Pharm Pharmacol. 2013;65(2):157–70. [PubMed: 23278683]
33. Pommier Y, Leo E, Zhang H, Marchand C. DNA topoisomerases and their poisoning by anticancer and antibacterial drugs. Chem Biol. 2010;17(5):421–33. [PubMed: 20534341]
34. Dunkern TR, Wedemeyer I, Baumgartner M, Fritz G, Kaina B. Resistance of p53 knockout cells to doxorubicin is related to reduced formation of DNA strand breaks rather than impaired apoptotic signaling. DNA Repair (Amst). 2003;2(1):49–60. [PubMed: 12509267]
35. Wang D, Lippard SJ. Cellular processing of platinum anticancer drugs. Nat Rev Drug Discov. 2005;4(4):307–20. [PubMed: 15789122]
36. Lakin ND, Jackson SP. Regulation of p53 in response to DNA damage. Oncogene. 1999;18(53): 7644–55. [PubMed: 10618704]
37. Kafer GR, Li X, Horii T, Suetake I, Tajima S, Hatada I, et al. 5-Hydroxymethylcytosine Marks Sites of DNA Damage and Promotes Genome Stability. Cell Rep. 2016;14(6):1283–92. [PubMed: 26854228]
38. Mizushima N Autophagy: process and function. Genes Dev. 2007;21(22):2861–73. [PubMed: 18006683]
39. Muller PA, Vousden KH. Mutant p53 in cancer: new functions and therapeutic opportunities. Cancer Cell. 2014;25(3):304–17. [PubMed: 24651012]
40. Liang SH, Clarke MF. Regulation of p53 localization. Eur J Biochem. 2001;268(10):2779–83. [PubMed: 11358492]
41. Boyd SD, Tsai KY, Jacks T. An intact HDM2 RING-finger domain is required for nuclear exclusion of p53. Nat Cell Biol. 2000;2(9):563–8. [PubMed: 10980695]
42. Lian CG, Xu Y, Ceol C, Wu F, Larson A, Dresser K, et al. Loss of 5-hydroxymethylcytosine is an epigenetic hallmark of melanoma. Cell. 2012;150(6):1135–46. [PubMed: 22980977]
43. Jiang D, Wei S, Chen F, Zhang Y, Li J. TET3-mediated DNA oxidation promotes ATR-dependent DNA damage response. EMBO Rep. 2017;18(5):781–96. [PubMed: 28325772]
44. Dou Z, Xu C, Donahue G, Shimi T, Pan JA, Zhu J, et al. Autophagy mediates degradation of nuclear lamina. Nature. 2015;527(7576):105–9. [PubMed: 26524528]

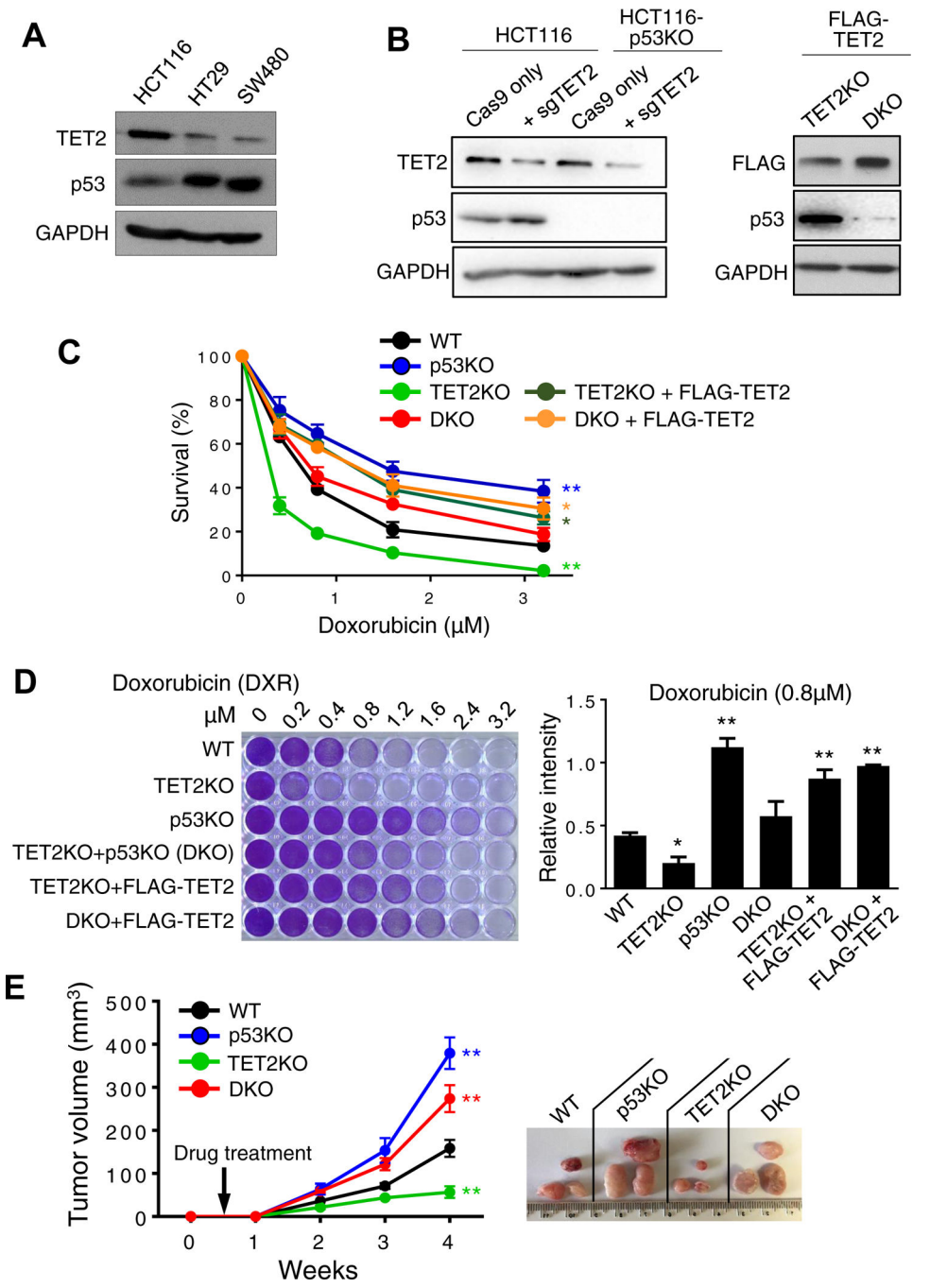

Figure 1. TET2 depletion overcomes anti-cancer treatment resistance in p53-null HCT116 cells.

(A) Endogenous levels of TET2 and p53 proteins in colon cancer cell lines (HCT116, HT29 and SW480). GAPDH was used as loading control.

(B) (Left) TET2 and p53 protein expression levels in WT and p53KO HCT116 cells treated with and without sgRNA to deplete endogenous TET2. (Right) FLAG-TET2 and p53 protein expression levels in TET2KO and p53KO+TET2KO (DKO) HCT116 cells with over-expression of FLAG-TET2.

(C) Assessment of cell viability. WST-1 was used to measure the percentage of survived HCT116 cells (WT, p53KO, TET2KO, p53KO+TET2KO (DKO), TET2KO + FLAG-TET2, and DKO + FLAG-TET2) after incubation with increasing doses (0, 0.4, 0.8, 1.6, 3.2 μM) of doxorubicin for 48 hrs (n = 3 independent experiments). Data were shown as mean ± S.D.; * $p < 0.01$, ** $p < 0.001$ (two-tailed Student's t-test compared with WT).
(D) Colony forming assay to measure the viability of HCT 116 cells (WT, p53KO, TET2KO, p53KO+TET2KO (DKO), TET2KO+FLAG-TET2, DKO+FLAG-TET2) treated with different amounts (0, 0.2, 0.4, 0.8, 1.2, 1.6, 3.4, 3.2 μM) of doxorubicin for 60 hrs. (Left) Representative images showing the colony forming assay result; (Right) quantifications of colony formation (n = 3 independent experiments). Data were shown as mean ± S.D.; * $p < 0.01$, ** $p < 0.001$ (two-tailed Student's t-test compared with WT).
(E) Tumor volume (left) and representative images (right) at the indicated time points in nude mice that were orthotopically implanted with corresponding HCT 116 tumor cells. n = 3 mice / group. ** $p < 0.001$ (two-tailed Student's t-test compared with WT).

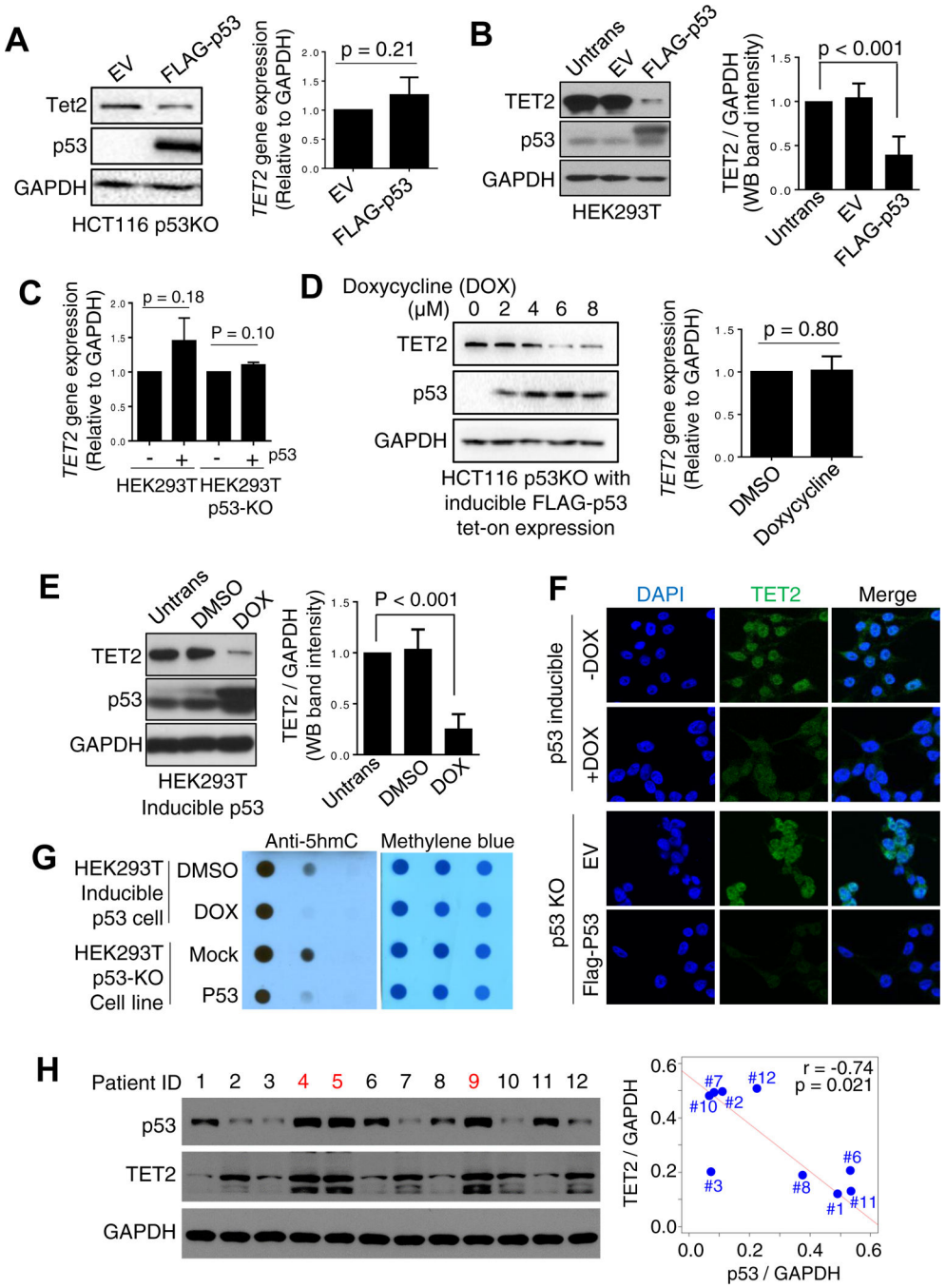

Figure 2. p53 downregulates TET2 at protein level, but not at mRNA level.

(A) (Left) Western-blotting analysis on TET2 and p53 protein levels in p53KO HCT 116 cells with and without re-expressing FLAG-tagged p53. (Right) Quantification of band intensities of western-blotting results (n = 3 independent experiments). Data were shown as mean ± S.D.

(B) (Left) Western-blotting analysis on TET2 and p53 protein levels in HEK293T cells without transfection, transfected with empty vector (EV) or FLAG-tagged p53. (Right)

Quantification of band intensities of western-blotting results (n = 3 independent experiments). Data were shown as mean ± S.D.

(C) Real-time quantitative PCR analysis of TET2 mRNA. (n = 3 independent experiments). Data were shown as mean ± S.D. (two-tailed Student's t-test).

(D) (Left) Western-blotting to monitor TET2 and p53 protein levels in p53KO HCT 116 cells with inducible expression of p53 following the addition of increasing doses of doxycycline (0, 2, 4, 6, 8 μM). (Right) Real-time quantitative PCR analysis of TET2 mRNA in corresponding experimental groups. (n = 3 independent experiments). Data were shown as mean ± S.D. (two-tailed Student's t-test).

(E) (Left) Western-blotting for monitoring TET2 and p53 protein levels in HEK293T cells in the indicated experimental groups. (Right) Quantification of band intensities of western-blotting results (n = 3 independent experiments). Data were shown as mean ± S.D.

(F) Representative confocal images of HEK293T cells stained with DAPI (blue, nuclei) and an anti-TET2 antibody (green) in the indicated experimental groups. Doxycycline was added to induce the expression of p53. EV, empty vector

(G) Representative dotblot assay results showing the measurement of the global 5hmC levels in HEK293T cells (with doxycycline inducible expression of p53; top two panels) or in p53KO HEK293T cells (lower two panels). Shown on the right is the methylene blue staining results to ensure equal loading of total DNA.

(H) (Left) Western-blotting analysis on p53 and TET2 in tumor samples collected from patients with colon cancer. Patients 4, 5 and 9 had p53 miss-sense mutations. (Right) Scatter plot of normalized p53 and TET2 (normalized to GAPDH) protein levels in individual patient with WT p53. Person correlation coefficient was calculated ($r = -0.74$ and $p = 0.021$).

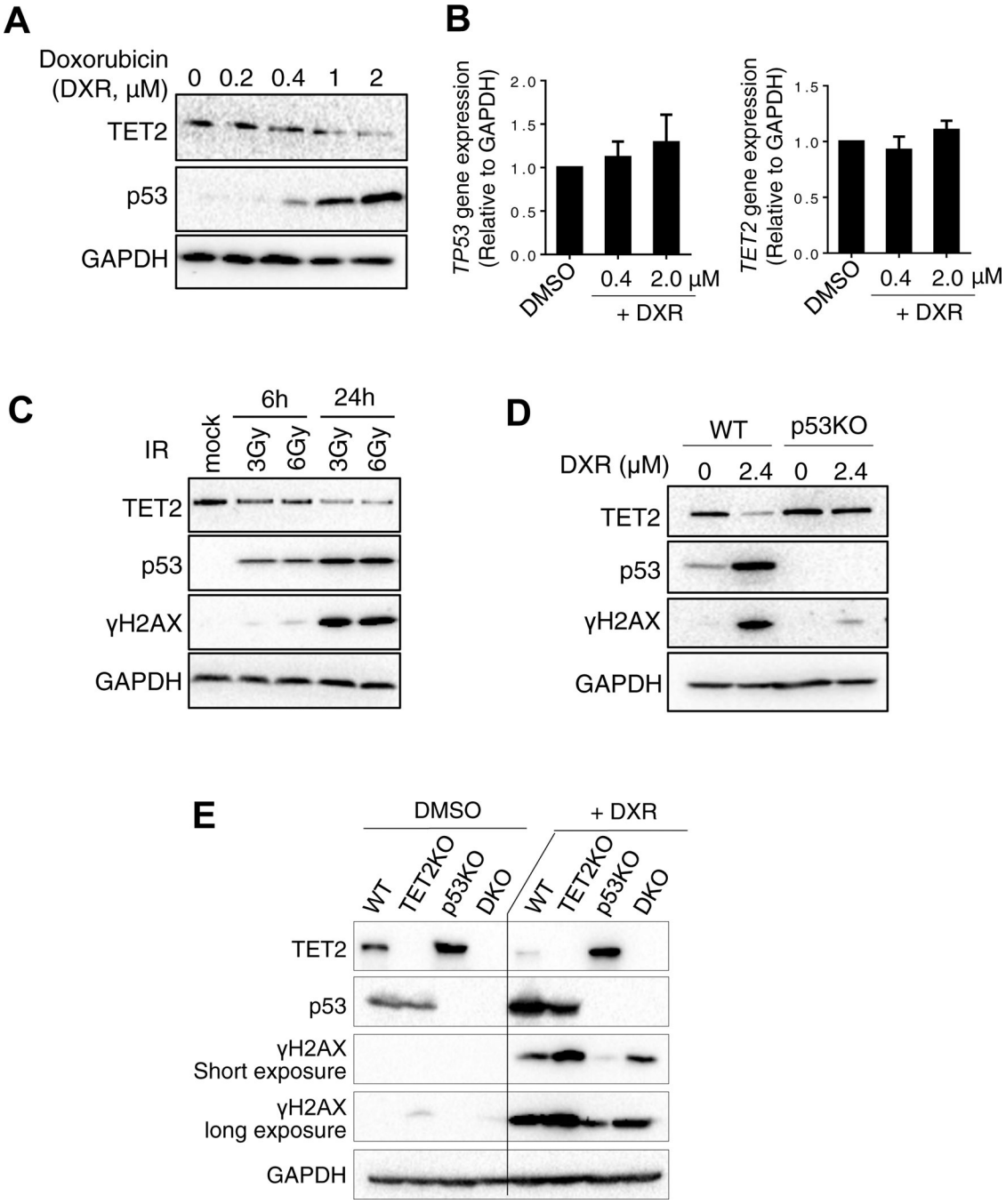

Figure 3. A negative correlation between p53 and TET2 protein levels in response to anti-cancer treatment with doxorubicin.

(A) Western-blotting analysis on TET2 and p53 protein levels in HCT116 cells treated with increasing doses (0, 0.2, 0.4, 1, 2 μM) of doxorubicin for 24 hrs.

(B) mRNA expression levels of *TET2* and *TP53* measured by qPCR in HCT116 cells treated with DMSO or doxorubicin (0.4 and 2.0 μM) for 24 hrs (n = 3 independent experiments). Data were shown as mean ± S.D.

(C) Western-blotting analysis on TET2, p53 and γH2AX protein levels in HCT116 cells exposed to 3 or 6 Gy gamma irradiation for 6 or 24 hrs, respectively.

(D) Western-blotting analysis on TET2, p53 and γH2AX protein levels in WT and p53KO HCT 116 cells treated with 0 or 2.4 μM doxorubicin for 24 hrs, respectively.
(E) Western-blotting analysis on TET2, p53 and γH2AX protein levels in WT, TET2KO, p53KO, and TET2KO+p53KO (DKO) cells treated with DMSO (control) or 2.4 μM doxorubicin for 24 hrs.

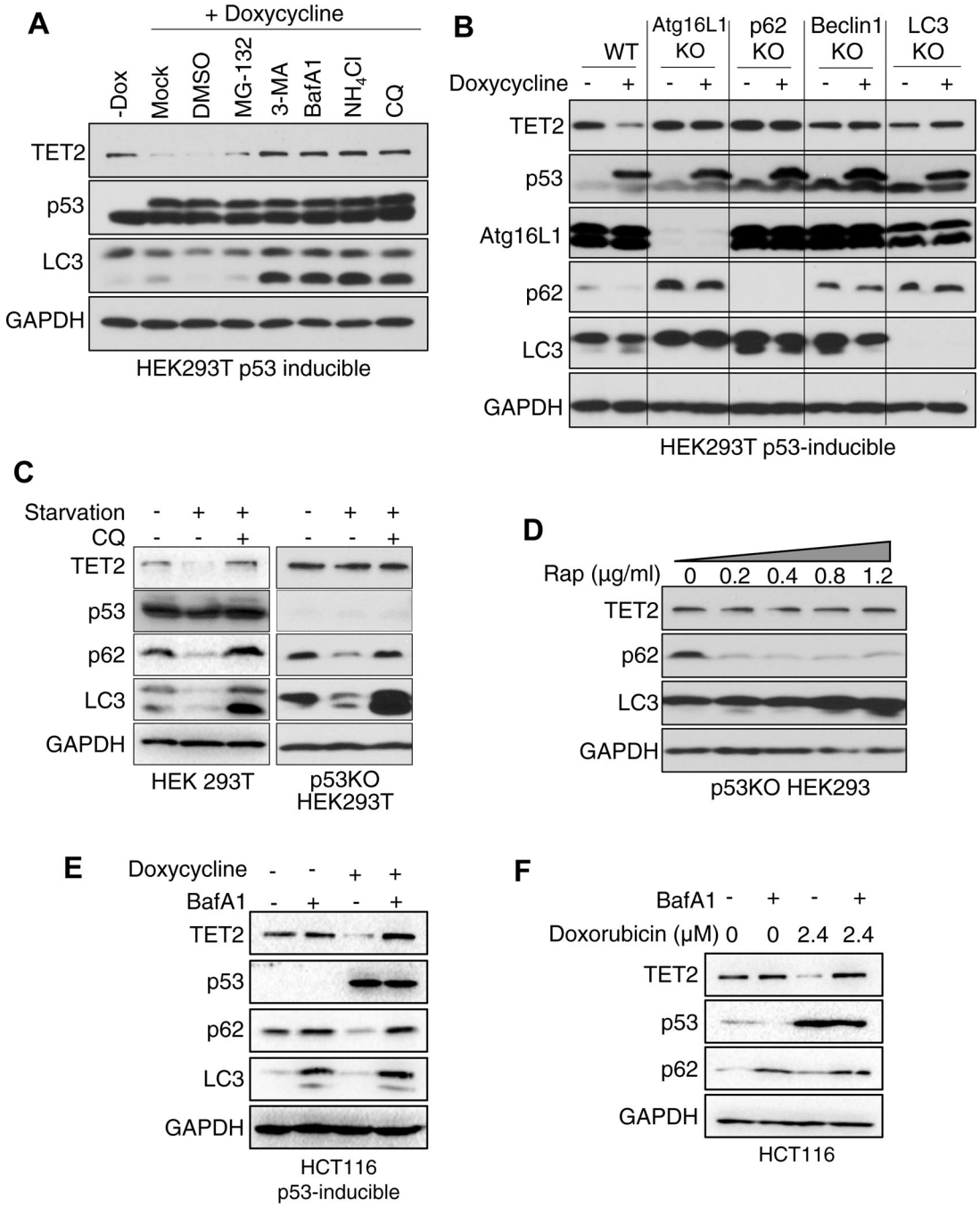

Figure 4. p53 downregulates TET2 through autophagic degradation.

(A) Western-blotting analysis on TET2, p53 and LC3 in HEK293T cells with doxycycline inducible expression of p53 in the presence of corresponding inhibitors. MG-132 were used to suppress proteosomal degradation whereas 3-MA, BafA1, NH_4Cl and CQ were added to inhibit autophagy (MG-132: 10 μM; 3-MA: 10 mM; BafA1: 25 nM; NH_4Cl: 5 mM; CQ: 25 μM).

(B) Western-blotting to monitor TET2, p53, Atg16L1 and LC3 levels in p53-inducible HEK293T cells with or without depletion of the indicated autophagy-related genes.

(C) Western-blotting analysis on TET2, p53 and autophagy-related proteins (p62 and LC3 in WT and p53KO HEK293T cells under the indicated culture conditions (i.e., serum-free starvation and/or autophagy inhibitor treatment with 25 μM chloroquine, CQ).
(D) Endogenous TET2, p62 and LC3 protein levels in p53KO HEK293T cells treated with increasing doses of rapamycin (0, 0.2, 0.4, 0.8, 12 μg/ml) for 24 hrs.
(E) Western-blotting analysis on TET2, p53, p62 and LC3 in p53-inducible HCT116 cells with and without bafilomycin A1 (BafA1) treatment (25 nM for 24 hrs). Doxycycline was added to induce p53 expression.
(F) Western-blotting analysis on TET2, p53, p62 and LC3 in WT HCT 116 cells with and without bafilomycin A1 (BafA1) treatment (25 nM for 24 hrs) together with doxorubicin treatment for 24 hrs. Doxorubicin was added to induce cellular stress and p53 upregulation (see Figure 3A).

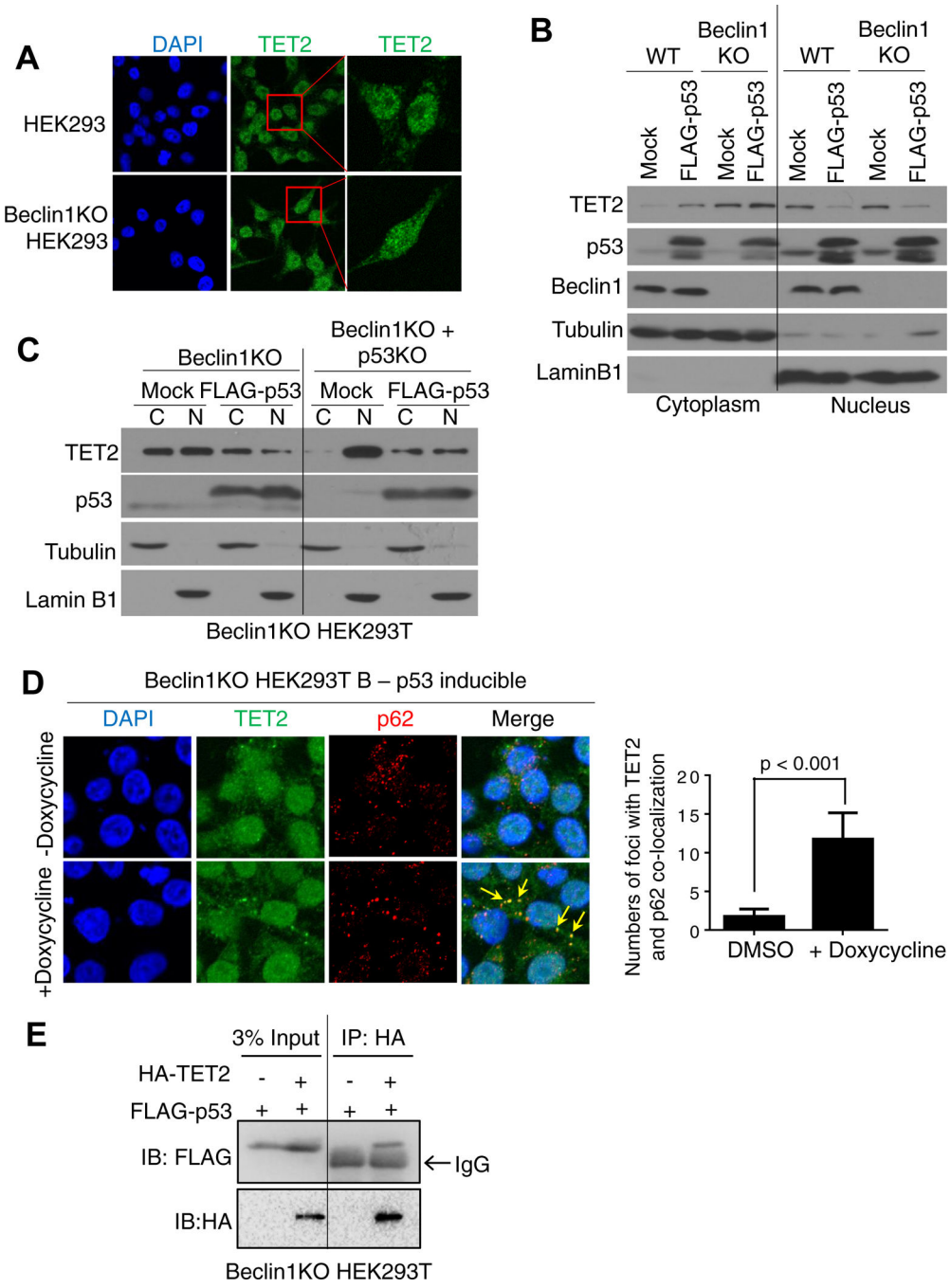

Figure 5. p53 is required for the autophagic degradation of TET2.

(A) Confocal images of native (upper) or Beclin 1 knockout (Beclin1KO; lower) HEK293T cells stained for visualization of TET2 (green) and the nuclei (DAPI).

(B) Western-blotting analysis on the cytoplasmic and nuclear fractions of TET2, p53, Beclin1 in WT and beclin1KO HEK293T cells with and without expression of FLAG-tagged p53.

(C) Western-blotting analysis on the cytoplasmic (C) and nuclear (N) fractions of TET2, p53 in Beclin1 KO or becklin1KO+p53KO (DKO) HEK293T cells with or without expression of FLAG-tagged p53.

(D) Confocal images showing the distribution of TET2 (green) and p62 (red) in beclin1 KO HEK293T cells before (upper) and after (lower) inducible expression of p53. DAPI was used to visualize the nuclei. Shown on the right is the quantification of colocalization of TET2 and p62 (n = 68). Doxycycline as added to induce p53 expression.

(E) Co-immunoprecipitation (co-IP) confirmed the interaction between p53 and TET2 in beclin1KO HEK293T cells.

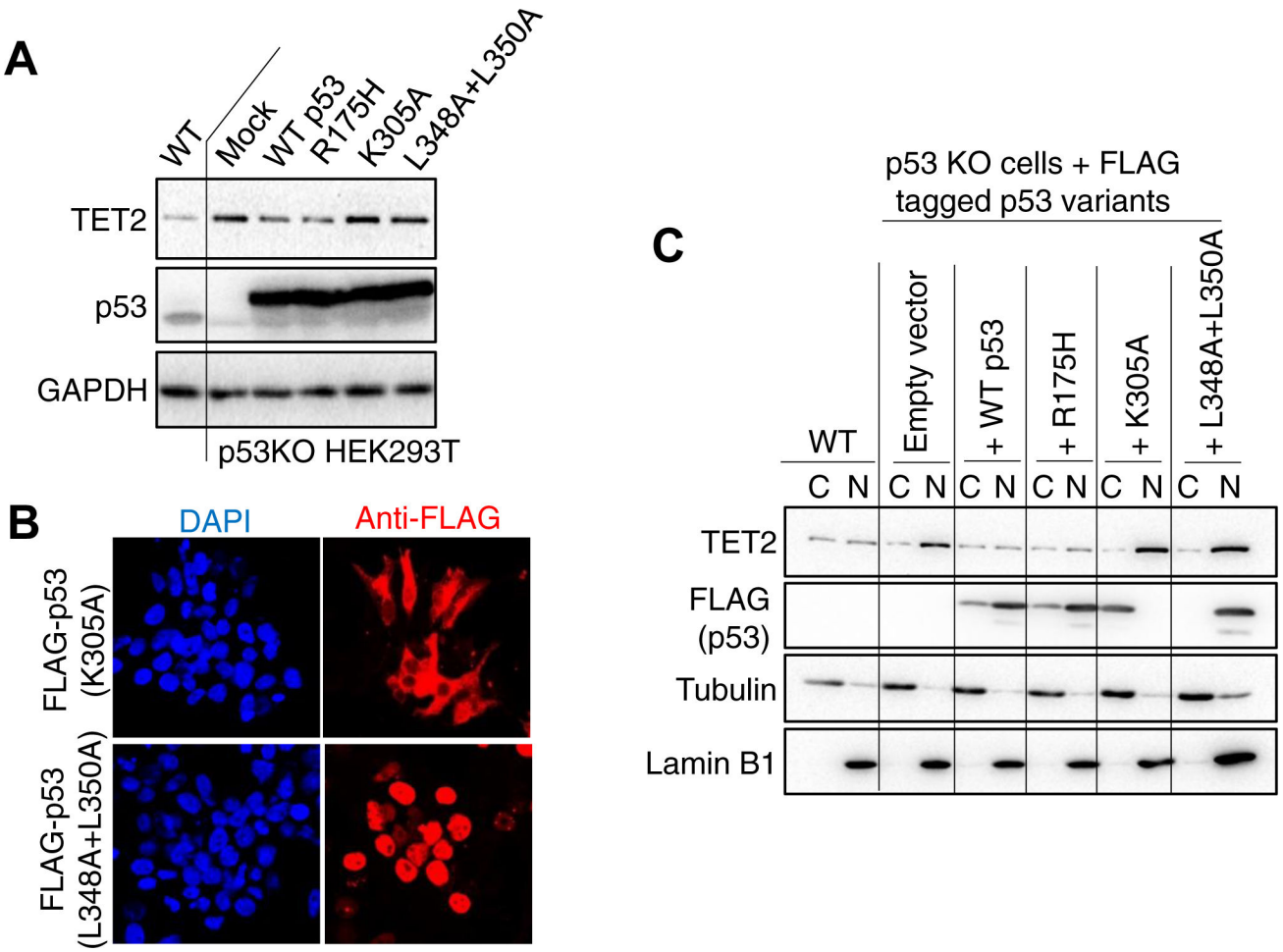

Figure 6. p53 mutations impair autophagy-mediated TET2 degradation.

(A) Western-blotting analysis on TET2 and p53 in p53KO HEK293T cells expressing WT and the indicated p53 mutants. K305A and L348A/L350A, but not R175H, are known to cause either cytosolic or nuclear retention of p53 proteins.

(B) Confocal images showing the subcellular localization of FLAG-tagged p53 mutants (red). Nuclei were stained with DAPI and shown in blue.

(C) Western-blotting analysis on the cytoplasmic and nuclear fractions of TET2 and p53 in p53KO HEK293T cells expressing WT or the indicated FLAG-tagged p53 mutants. Tubulin and lamin B1 were used to indicate the separation of cytosolic (C) and nuclear (N) fractions, respectively.

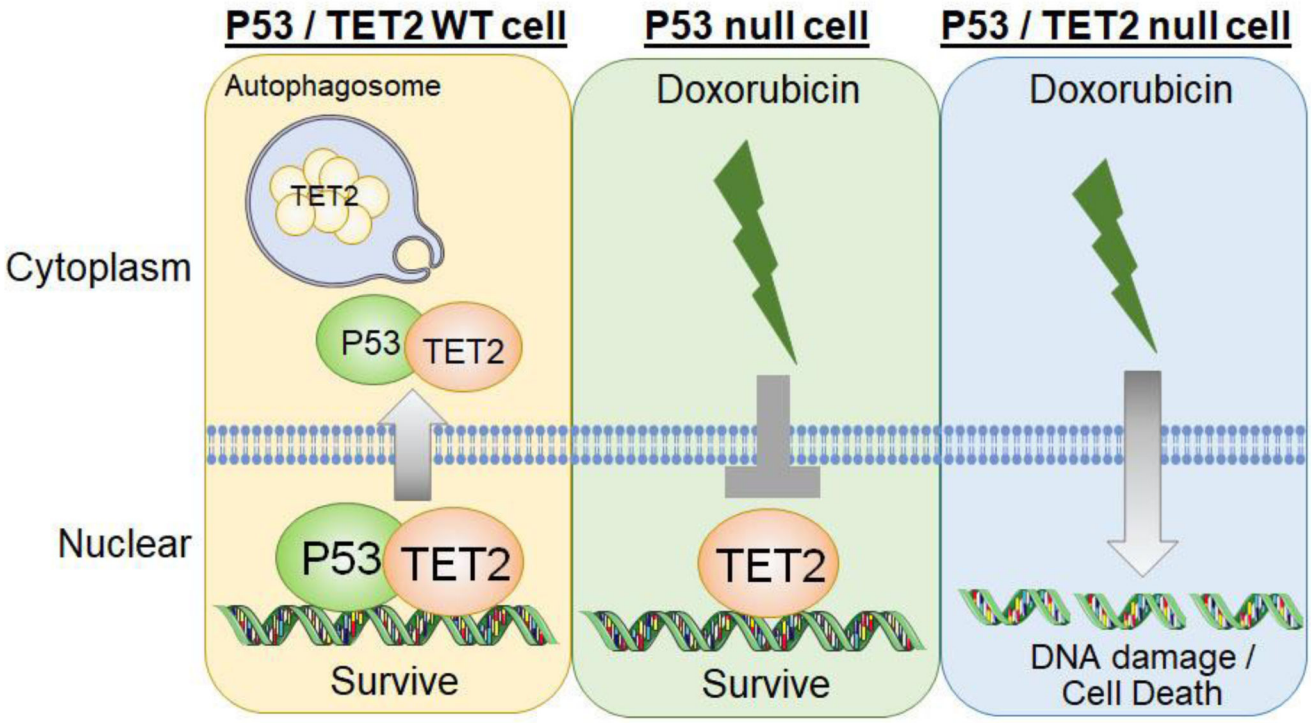

Figure 7. A tentative model depicting how chemotherapy (doxorubicin) disrupts the p53-associated autophagic degradation of TET2 in p53-null tumor cells.

(Left) In WT cells, p53 facilitates the autophagic degradation of TET2 through enhancing the TET2 nuclear exit with subsequent recruitment toward the autophagosome. A balance of p53 and TET2 is needed to maintain the normal cellular function. (Middle) In p53 KO cells, p53 loss leads to less TET2 protein degradation in the cytosol but more accumulation in the nucleus during doxorubicin treatment. Nuclear TET2 protects the genome from DNA damage imposed by doxorubicin. This ultimately promotes tumor cell growth and survival, which contributes to the chemotherapy resistance. (Right) In p53KO and TET2KO (DKO) cells, the protective effect of TET2 is removed following chemotherapy induced DNA damage, thereby overcoming therapeutic resistance to restore tumor cell killing.